

Reduced field-of-view diffusion-weighted imaging (DWI) in patients with gastric cancer

Comparison with conventional DWI techniques at 3.0T: A preliminary study

Jin-Song Cai, MD^a, Hai-Yan Chen, MD^a, Jie-Yu Chen, MD^a, Yuan-Fei Lu, MD^a, Jian-Zhong Sun, MD^a, Ying Zhou, MD^b, Ri-Sheng Yu, MD, PhD^{a,*}

Abstract

To evaluate the qualitative image quality and quantitative apparent diffusion coefficient (ADC) value of reduced field-of view (rFOV) and full field-of-view (fFOV) diffusion-weighted imaging (DWI) sequences at 3.0 T in patients with gastric cancer.

Fifty-three patients (37 males, 16 females; mean age, 63.3±10.3 years) with 60 lesions with gastric cancer who underwent magnetic resonance (MR) scans, including both rFOV-DWI and fFOV-DWI, were retrospectively analyzed. Two observers subjectively evaluated image quality for both the fFOV-DWI and rFOV-DWI sequences regarding the anatomic details, distortion, lesion conspicuity, artifacts, and overall image quality. The mean ADC values of gastric cancer were calculated. The Wilcoxon test and paired samples *t* test were used. Interobserver agreement was assessed using kappa statistics.

The mean scores based on the 2 observers demonstrated significant differences in image quality in terms of anatomic details, distortion, lesion conspicuity, artifacts and overall image quality at both *b* values between rFOV-DWI and fFOV-DWI ($P < .05$) in the whole gastric area. rFOV-DWI yielded significantly better scores in image quality at $b = 800 \text{ seconds/mm}^2$ ($P < .05$) in patients with esophagogastric junction cancers, but there were no significant differences in the gastric corpus and gastric antrum region. The mean tumor ADC values of rFOV-DWI were significantly lower than those of fFOV-DWI ($1.237 \pm 0.228 \times 10^{-3} \text{ mm}^2/\text{second}$ vs $1.683 \pm 0.322 \times 10^{-3} \text{ mm}^2/\text{second}$, $P < .001$).

rFOV-DWI yielded significantly better image quality (anatomic details, distortion, lesion conspicuity, artifacts, overall image quality) and more accurate ADC measurements than fFOV-DWI did.

Abbreviations: ADC = apparent diffusion coefficient, DWI = diffusion-weighted imaging, EPI = echo-planar imaging, fFOV = full field-of-view, MR = magnetic resonance, rFOV = reduced field-of view, ROI = region of interest, T1WI = T1-weighted images, T2WI = T2-weighted images.

Keywords: magnetic resonance imaging, retrospective study, stomach neoplasms

Editor: Bülent Kantarçeken.

JSC and HYC contributed equally and should be considered as co-first authors.

The research was supported by Zhejiang Provincial program named construction of major disease diagnosis and treatment technology research center—gastric carcinoma, 17-2018-%s-0077.

The authors report no conflicts of interest.

^a Department of Radiology, ^b Department of Neurology, Second Affiliated Hospital, Zhejiang University School of Medicine, Hangzhou, China.

* Correspondence: Ri-Sheng Yu, Department of Radiology, Second Affiliated Hospital, Zhejiang University School of Medicine, Jiefang Road 88#, Hangzhou, 310009, China (e-mail: risheng-yu@zju.edu.cn).

Copyright © 2020 the Author(s). Published by Wolters Kluwer Health, Inc. This is an open access article distributed under the terms of the Creative Commons Attribution-Non Commercial License 4.0 (CCBY-NC), where it is permissible to download, share, remix, transform, and buildup the work provided it is properly cited. The work cannot be used commercially without permission from the journal.

How to cite this article: Cai JS, Chen HY, Chen JY, Lu YF, Sun JZ, Zhou Y, Yu RS. Reduced field-of-view diffusion-weighted imaging (DWI) in patients with gastric cancer: comparison with conventional DWI techniques at 3.0T: A preliminary study. *Medicine* 2020;99:1(e18616).

Received: 16 June 2019 / Received in final form: 8 November 2019 / Accepted: 5 December 2019

<http://dx.doi.org/10.1097/MD.00000000000018616>

1. Introduction

Gastric cancer is the fifth most common malignancy worldwide and the leading cause of cancer mortality in Eastern Asia.^[1] Currently, therapeutic strategies range from endoscopic mucosal resection to neoadjuvant chemotherapy due to preoperative staging, making accurate preoperative staging a necessity.^[2,3]

Diffusion-weighted imaging (DWI) is a fundamental sequence frequently performed by the single-shot echo-planar imaging (EPI) technique, and it assesses aspects of the tissue microenvironment, such as cell membrane integrity, water mobility, and tissue cellularity.^[4-6] Gastric cancer presents with a higher cell density and restriction of water diffusion, resulting in a lower apparent diffusion coefficient (ADC) value than that of normal gastric tissue.^[4,7] Some studies have shown that the ADC can be an independent prognostic factor in gastric cancer patients and is relevant to various histopathologic features, such as the histologic grade and subtype and Ki67 cell proliferation index.^[7-9] However, in patients with gastric cancer, DWI scans are not routinely performed.^[4] The imaging quality of conventional full field-of-view (fFOV) DWI may be affected by obvious anatomic distortion, low spatial resolution, and susceptibility artifacts because of B₀-field inhomogeneities, very short acquisition times, and eddy

currents.^[6,10] Gas and gastric movement may exacerbate such artifacts leading to image distortion and ghosting.^[6] Thus, high-resolution DWI scans of the gastric region may be needed to some extent, and may also be valuable in identifying gastric cancers.

Recently, an attractive technical advancement in EPI acquisition named reduced field-of-view (rFOV) DWI has been introduced.^[11] The rFOV-DWI technique uses a 2D spatially selective excitation pulse to excite a limited FOV along the phase-encoding direction by reducing the number of required k-space lines.^[12,13] This technique enables shorter readout times to reduce distortion artifacts and images with a higher resolution.^[14] This technique has achieved high-resolution images of the spinal cord, prostate, breast, heart, kidney, pancreas, thyroid gland, optic nerve, rectal, uterus, head, and neck.^[6,12,15–23] However, to the best of our knowledge, the application of rFOV-DWI in the gastric region has not been reported thus far. Therefore, this retrospective and preliminary study aimed to compare image qualities and ADC values of gastric cancers between rFOV-DWI and fFOV-DWI 3.0T magnetic resonance (MR) scans.

2. Methods

2.1. Patients

This retrospective study was approved by our medical ethics committee, and the requirement for obtaining informed consent from all patients was waived. Fifty-three consecutive patients who underwent 3.0 Tesla MR imaging scans for gastric cancer between December 2017 and July 2018 were retrospectively analyzed. The inclusion criteria for the patients were as follows:

- (1) diagnosis of gastric cancer confirmed by surgery resection or endoscopy guided biopsy;
- (2) lesions with locations confirmed by gastroscopy before an MRI examination was performed; and
- (3) both fFOV-DWI and rFOV-DWI results.

2.2. MR image acquisition

All MR images were acquired using a 3.0-T system (Discovery MR750; GE Healthcare, Waukesha, WI) with a 32-channel torso-array coil in the supine position. All patients were asked to fast from solid food 4 to 6 hours before the examination. Gastric cavity distension was acquired by oral administration of 800 mL to 1000 mL of water within 5 minutes before the MR imaging scan. The patients were instructed on how to breathe appropriately before the examination. Unless contraindicated, 40 mg of NO-SPA was injected intramuscularly (drotaverine hydrochloride injection; Csanyikvolgy, Hungary) to prevent gastrointestinal motility 15 minutes before image acquisition.

The routine MR sequence included axial Lava Flex T1-weighted images (T1WI) and fat-saturated T2-weighted images (T2WI), conventional fFOV-DWI and rFOV-DWI, and dynamic axial contrast-enhanced T1WI, coronal Lava Flex T1-weighted images (T1WI).

The imaging parameters for the 3D T1WI were as follows: a repetition time/echo time (TR/TE) of 3.8/1.7 ms, standard field-of-view of 380 mm, slice thickness of 4 mm without any slice spacing, and matrix size of 320 × 224. The fat-saturated T2WI were performed using PROPELLER technology with respiratory triggering, a repetition time/echo time (TR/TE) of 12,000/93 ms, a field-of-view of 360 mm, a slice thickness of 5 mm, a slice spacing size of 1.0 mm, and a matrix size of 320 × 320. For the contrast-enhanced T1WI (Omniscan, 0.1 mmol/kg body weight; GE

Healthcare), the arterial phase, portal venous phase, equilibrium phase and delayed phase images (18–19, 40–50, 90 and 180–300 seconds after the injection, respectively) were collected separately under dynamic breath-hold T1WI acquisitions.

Conventional fFOV-DWI scans were performed using respiratory-triggered single-shot EPI techniques with fat suppression in the axial plane. Two *b* values (0 and 800 seconds/mm²) were included. The scanning parameters were as follows: TR/TE, 6000 ms/75 ms; slice thickness, 5 mm; slice spacing, 1 mm; flip angle, 90°; FOV, 360 mm × 360 mm; matrix size, 128 × 160; NEX, 12; bandwidth, 250 kHz; respiratory rate, updated to real time (approximately 18) and acquisition time, 1 minute, 24 seconds. The in-plane spatial resolution was 2.81 × 2.25 mm².

Since the small FOV could not completely cover the entire stomach, we divided the stomach into three regions according to the location of the lesion. Additionally, the lesion was always in the center of the rFOV-DWI scan, and the long axis of the lesion was parallel with the long axis of the small FOV in the scan. The rFOV-DWI scans were performed with *b* values of 0 and 800 seconds/mm². A 2D spatially selective radiofrequency pulse and 180° refocusing pulse were used to reduce the FOV in the phase-encoded direction with fat suppression. The scanning parameters were as follows: TR/TE, 6000 ms/75 ms; slice thickness, 5 mm; slice spacing, 0 mm; flip angle, 90°; FOV, 180 mm × 90 mm; matrix size, 128 × 64; NEX, 10; bandwidth, 250 kHz; respiratory rate, updated to real time (approximately 18) and acquisition time, 3 minutes, 33 seconds. The in-plane spatial resolution was 1.40 × 1.40 mm² (Table 1).

3. Image analysis

3.1. Qualitative image analysis

The qualitative assessments were performed independently by 2 board-certified abdominal radiologists (with 15 and 30 years of experience) at a standard PACS (iSite, Philips Healthcare). Two observers subjectively evaluated image quality for both the fFOV-DWI and the rFOV-DWI sequences regarding the anatomic details (the ability to identify the gastric anatomic details), distortion (degree of image distortion), lesion conspicuity (visibility of lesions), artifacts (respiratory motion artifacts and magnetic susceptibility artifacts, as well as other artifacts such as noise, blurring and signal drop), and overall image quality, while using the T2-weighted images as a reference. To minimize recognition bias, the patients were randomly divided into 2 groups (1 and 2). First, the observers either assessed both the rFOV-DWI results and T2WI in group 1 or assessed both the fFOV-DWI results and T2WI in group 2. In addition, the order of the patients was randomized

Table 1
Imaging parameters for reduced field of view (rFOV) diffusion weighted imaging (DWI) and full field of view (fFOV) DWI.

Sequence parameter	rFOV-DWI	fFOV-DWI
TR/TE (msec)	6000/75	6000/75
Slice thickness/spacing (mm)	5/0	5/1
Flip angle	90°	90°
FOV (mm)	180 × 90	360 × 360
Matrix	128 × 64	128 × 160
NEX	10	12
Bandwidth (kHz)	250	250
Resolution	1.40 × 1.40	2.81 × 2.25
Acquisition time	3 min, 33 s	1 min, 24 s
B-value (s/mm ²)	0, 800	0, 800

within the 2 groups. Second, the same assessment was implemented after the groups were switched. Moreover, these 2 parts of the assessment occurred at least 2 weeks apart to minimize recall bias.

The 5-point quality scales using a Likert scale that were used for evaluating image quality were as follows:

- (1) anatomic detail: 1 = very poor, poorly visualized anatomy and nondiagnostic; 2 = poor, gastric contour and margin blurred; 3 = inconclusive, fairly delineated stomach with margin blurring; 4 = good, good delineation of stomach with a sharp margin; 5 = excellent, excellent sharpness of the stomach;
- (2) distortion: 1 = very poor; 2 = severe; 3 = moderate; 4 = slight; 5 = no distortion;
- (3) lesion conspicuity: 1 = not recognizable; 2 = slight signal difference; 3 = moderate signal difference; 4 = distinct signal difference; 5 = distinct signal difference with a clear lesion margin;
- (4) artifacts: 1 = very poor; 2 = severe; 3 = moderate; 4 = mild; 5 = absent;
- (5) overall image quality: 1 = very poor; 2 = poor; 3 = inconclusive; 4 = good; 5 = excellent.

For each DWI sequence, the $b=0$ seconds/mm² images were reviewed and evaluated first, followed by the $b=800$ seconds/mm² images.

3.2. Quantitative image analysis

The ADC values were calculated by drawing regions of interest (ROIs) on the ADC maps on a workstation (aw4.6; GE Healthcare) and were measured quantitatively by one radiologist (with 7 years of experience in abdominal radiology). The ROIs was drawn to cover as much of the tumor tissue as possible in the maximum dimension of the tumor. Meanwhile, T2WI were used to identify regions of necrosis, vessels, and gastric fluid, which need to be avoided to minimize bias. The ADC values were acquired twice in the same position, and the average value was recorded.

3.3. Statistical analysis

The readers' qualitative image analysis scores were compared by the Wilcoxon signed ranks test between rFOV-DWI and fFOV-DWI. In addition, the three locations of the stomach (esophagogastric junction, gastric corpus, and gastric antrum) were analyzed separately. The gastric corpus is in the middle of the stomach along the curvature. Interobserver agreement for the qualitative evaluations was assessed using kappa statistics. A kappa value of less than 0.20 shows poor agreement, a value of 0.21 to 0.40 shows fair agreement, a value of 0.41 to 0.60 shows moderate agreement, a value of 0.61 to 0.80 shows good agreement, and a value greater than 0.81 shows excellent agreement. Mean ADC values of gastric cancer were compared between the two DWI sequences using the paired samples *t* tests. All tests were two-sided, and *P* values <.05 were considered statistically significant. All statistical analyses were performed with SPSS V.23.0 (SPSS Inc., an IBM company, Chicago, IL).

4. Results

Fifty-three patients with 60 lesions were enrolled in our research, including 37 males and 16 females (mean age, 63.3 ± 10.3 years, range, 44–84 years). In total, 21 lesions were diagnosed as esophagogastric junction cancers, 22 lesions were diagnosed as gastric corpus cancers, and 17 lesions were diagnosed as gastric antrum cancers by surgery or endoscopy guided biopsy.

There were 53 lesions (53/60, 88.3%) detected by rFOV-DWI, and the tumor size was 4.29 ± 1.97 cm; 49 lesions (49/60, 81.7%) were detected by fFOV-DWI, and the tumor size was 4.33 ± 2.05 cm. However, the tumor size was not different between these 2 groups ($P > .05$).

4.1. Qualitative analysis

Table 2 shows the rFOV-DWI and fFOV-DWI scores from the qualitative analysis. For both observers, rFOV-DWI attained

Table 2

Comparison of qualitative analysis scores between reduced field of view (rFOV) diffusion weighted imaging (DWI) and full field of view (fFOV) DWI of gastric carcinoma.

	Anatomic detail	Distortion	Lesion conspicuity	Artifacts	Overall image quality
Observer 1					
rFOV-DWI ($b=0$ s/mm ²)	3.07 ± 0.90	3.23 ± 0.91	2.65 ± 1.09	3.20 ± 0.80	3.23 ± 0.91
fFOV-DWI ($b=0$ s/mm ²)	2.87 ± 1.07	3.00 ± 0.88	2.33 ± 1.02	2.92 ± 0.96	3.00 ± 1.15
<i>P</i> value	.077	.032	.005	.044	.023
rFOV-DWI ($b=800$ s/mm ²)	3.55 ± 1.00	3.83 ± 0.98	3.83 ± 1.15	3.97 ± 0.84	4.03 ± 0.92
fFOV-DWI ($b=800$ s/mm ²)	3.32 ± 0.95	3.55 ± 0.72	3.53 ± 1.19	3.53 ± 0.83	3.57 ± 0.81
<i>P</i> value	.047	.022	.049	.001	<.001
Observer 2					
rFOV-DWI ($b=0$ s/mm ²)	3.08 ± 0.91	3.33 ± 0.97	2.72 ± 1.18	3.25 ± 0.80	3.13 ± 0.89
fFOV-DWI ($b=0$ s/mm ²)	2.93 ± 1.03	3.07 ± 1.06	2.47 ± 1.13	2.92 ± 0.94	2.92 ± 1.06
<i>P</i> value	.159	.019	.035	.013	.036
rFOV-DWI ($b=800$ s/mm ²)	3.52 ± 1.03	3.90 ± 0.97	3.85 ± 1.14	3.88 ± 0.94	3.90 ± 0.92
fFOV-DWI ($b=800$ s/mm ²)	3.25 ± 0.88	3.55 ± 0.79	3.45 ± 1.12	3.48 ± 0.87	3.70 ± 0.87
<i>P</i> value	.035	.013	.006	.003	.041
Mean					
rFOV-DWI ($b=0$ s/mm ²)	3.08 ± 0.83	3.28 ± 0.92	2.68 ± 1.12	3.23 ± 0.77	3.18 ± 0.88
fFOV-DWI ($b=0$ s/mm ²)	2.90 ± 0.99	3.03 ± 0.84	2.40 ± 1.04	2.92 ± 0.92	2.96 ± 1.08
<i>P</i> value	.044	.005	.022	.018	.023
rFOV-DWI ($b=800$ s/mm ²)	3.53 ± 0.99	3.87 ± 0.92	3.84 ± 1.11	3.93 ± 0.85	3.97 ± 0.89
fFOV-DWI ($b=800$ s/mm ²)	3.28 ± 0.86	3.55 ± 0.70	3.49 ± 1.15	3.51 ± 0.82	3.63 ± 0.81
<i>P</i> value	.025	.008	.005	.001	.001

Data are mean ± standard deviation.

Table 3**Comparison of qualitative analysis scores between reduced field of view (rFOV) diffusion weighted imaging (DWI) and full field of view (fFOV) DWI of 3 parts of gastric cancer.**

	Anatomic detail	Distortion	Lesion conspicuity	Artifacts	Overall image quality
Esophagogastric junction cancer					
rFOV DWI ($b=0$ s/mm ²)	3.26±0.60	3.60±0.74	2.90±1.03	3.33±0.51	3.52±0.70
fFOV DWI ($b=0$ s/mm ²)	3.14±0.88	3.19±0.81	2.50±1.12	3.00±0.84	3.05±1.04
<i>P</i> value	.422	.011	.132	.142	.006
rFOV DWI ($b=800$ s/mm ²)	3.81±0.87	4.14±0.84	4.02±0.90	4.12±0.79	4.17±0.70
fFOV DWI ($b=800$ s/mm ²)	3.45±0.88	3.45±0.65	3.48±1.17	3.33±0.86	3.43±0.58
<i>P</i> value	.039	.010	.013	.005	.001
Gastric corpus cancer					
rFOV DWI ($b=0$ s/mm ²)	3.16±0.71	3.07±0.97	2.68±0.88	3.36±0.80	3.14±0.68
fFOV DWI ($b=0$ s/mm ²)	2.84±1.04	3.00±0.65	2.52±0.87	2.89±0.99	3.14±1.05
<i>P</i> value	.046	.660	.332	.032	.942
rFOV DWI ($b=800$ s/mm ²)	3.55±0.84	3.73±0.87	3.80±1.12	3.86±0.85	3.98±0.81
fFOV DWI ($b=800$ s/mm ²)	3.30±0.68	3.66±0.76	3.52±1.17	3.77±0.72	3.84±0.71
<i>P</i> value	.052	.711	.118	.361	.207
Gastric antrum cancer					
rFOV DWI ($b=0$ s/mm ²)	2.74±1.11	3.18±1.00	2.41±1.46	2.91±0.94	2.82±1.19
fFOV DWI ($b=0$ s/mm ²)	2.68±1.03	2.88±1.07	2.12±1.15	2.85±0.96	2.62±1.15
<i>P</i> value	.599	.034	.041	.784	.221
rFOV DWI ($b=800$ s/mm ²)	3.18±1.21	3.71±1.06	3.68±1.33	3.76±0.94	3.71±1.15
fFOV DWI ($b=800$ s/mm ²)	3.06±1.03	3.53±0.70	3.47±1.17	3.38±0.84	3.62±1.11
<i>P</i> value	.751	.188	.460	.063	.521

Data are mean ± standard deviation.

significantly better scores in terms of anatomic details, distortion, lesion conspicuity, artifacts and overall image quality at both $b=0$ seconds/mm² and $b=800$ seconds/mm² than did fFOV-DWI ($P<.05$), but no significant differences were observed for anatomic details at $b=0$ s/mm² with both observers ($P=.077$, $.159$). Furthermore, the means of the scores from the 2 observers were calculated, and significant differences in image quality (anatomic details, distortion, lesion conspicuity, artifacts, and overall image quality) at both b values between rFOV-DWI and fFOV-DWI ($P<.05$) were found.

For the esophagogastric junction cancers, as Table 3 shows, the rFOV-DWI yielded significantly better scores in distortion and overall image quality at $b=0$ seconds/mm² ($P<.05$), and in anatomic detail, distortion, lesion conspicuity, artifacts and

overall image quality at $b=800$ seconds/mm² ($P<.05$). No significant differences were found in anatomic detail, lesion conspicuity or artifacts at $b=0$ seconds/mm² ($P=.422$, $.132$, $.142$, respectively), but the average rFOV-DWI scores were higher than the that of fFOV-DWI scores (Fig. 1).

For the gastric corpus cancers, as shown in Table 3, the mean rFOV-DWI score was higher than the fFOV-DWI score in the 5 aspects of image quality, except for overall image quality at $b=0$ seconds/mm², which was equal between 2 sequences. However, there were no obvious differences between rFOV-DWI and fFOV-DWI in these 5 aspects ($P>.05$), except in anatomic detail and artifacts at $b=0$ seconds/mm² ($P<.05$) (Fig. 2).

For the gastric antrum cancers, as shown in Table 3, the average rFOV-DWI scores were found to be superior to the

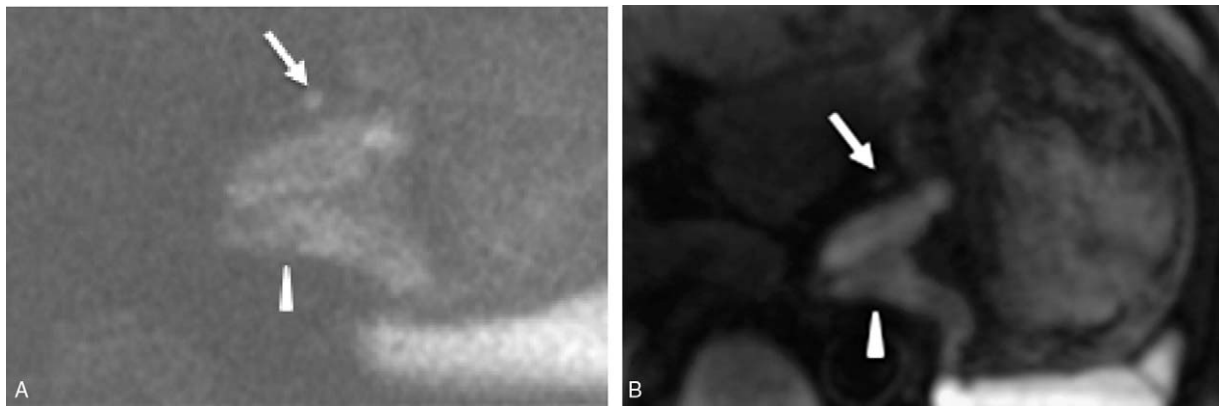


Figure 1. A 67-year-old man was diagnosed with esophagogastric junction cancer (middle-low differentiated adenocarcinoma). (A) The reduced field-of-view diffusion-weighted image (rFOV-DWI) ($b=800$ seconds/mm²) shows the thickening of the stomach wall at the esophagogastric junction (white arrowhead) with a clear edge, less distortion, and better overall image quality than the full field-of-view diffusion-weighted image (fFOV-DWI), which is shown in (B). Additionally, there is a small metastatic lymph node in picture A, but it is almost invisible in picture B (white arrow), indicating that rFOV-DWI has better lesion conspicuity than fFOV-DWI.

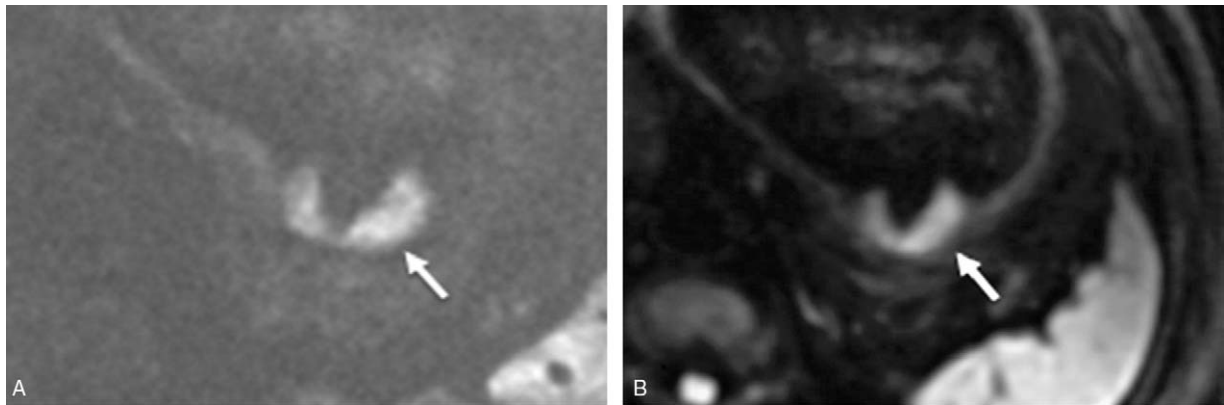


Figure 2. A 57-year-old man was diagnosed with gastric corpus cancer (middle-low differentiated adenocarcinoma). (A) The reduced field-of-view diffusion-weighted image (rFOV-DWI) ($b=800$ seconds/mm²) shows the irregular thickening of the stomach wall at the gastric corpus (white arrow) with a significantly clearer edge, less distortion, better lesion conspicuity and better overall image quality than full field-of-view diffusion-weighted image (fFOV-DWI), which is shown in (B).

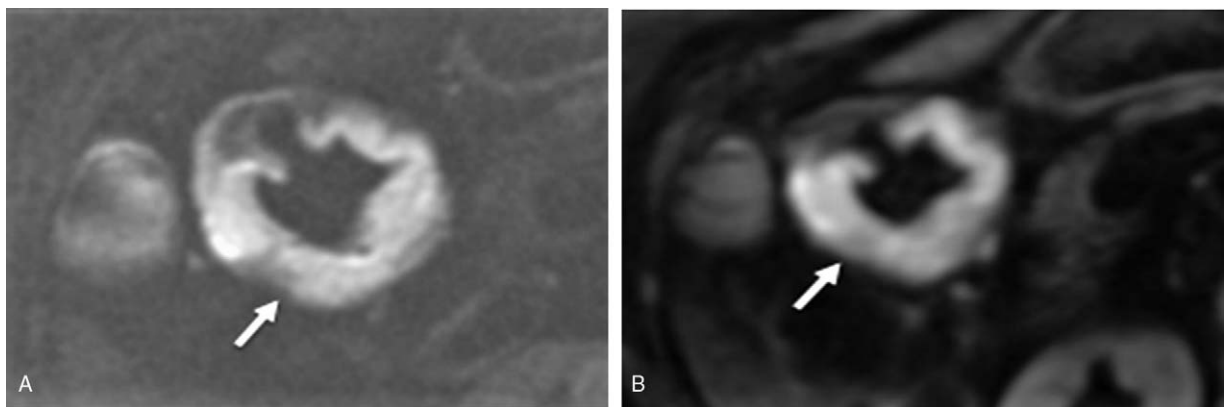


Figure 3. A 73-year-old woman was diagnosed with gastric antrum cancer (low differentiated adenocarcinoma). (A) The reduced field-of-view diffusion-weighted image (rFOV-DWI) ($b=800$ seconds/mm²) shows the obvious ring thickening of the stomach wall at the gastric antrum (white arrow) with a significantly clearer anatomic detail, less distortion, less artifacts, better lesion conspicuity, and better overall image quality than the full field-of-view diffusion-weighted image (fFOV-DWI), which is shown in (B).

fFOV-DWI scores in the 5 aspects of image quality. In addition, no significant difference was detected between rFOV-DWI and fFOV-DWI in these 5 aspects ($P>.05$), except in distortion and lesion conspicuity at $b=0$ seconds/mm² ($P<.05$) (Fig. 3).

Table 4 shows the interobserver agreement between the 2 observers for the qualitative analysis scores (anatomic detail, distortion, lesion conspicuity, artifacts, and overall image quality) for both b values. The interobserver agreement was poor to excellent in rFOV-DWI for anatomic detail, distortion, lesion conspicuity, artifacts, and overall image quality ($\kappa=0.400-0.891$

at $b=0$ seconds/mm² and $\kappa=0.541-0.745$ at $b=800$ seconds/mm²). Furthermore, there was fair to good agreement in fFOV-DWI for the 5 aspects of image quality ($\kappa=0.442-0.800$ at $b=0$ seconds/mm² and $\kappa=0.527-0.713$ at $b=800$ s/mm²).

4.2. Quantitative analysis

The mean tumor ADC values of rFOV-DWI were significantly lower than those of fFOV-DWI ($1.237 \pm 0.228 \times 10^{-3}$ mm²/second vs $1.683 \pm 0.322 \times 10^{-3}$ mm²/second, $P<.001$)

Table 4
Interobserver agreement of the qualitative analysis scores.

	Anatomic detail	Lesion Distortion	Lesion conspicuity	Presence of artifact	Overall image quality
rFOV-DWI ($b=0$ s/mm ²)	0.400 (0.216, 0.584)	0.760 (0.625, 0.895)	0.891 (0.801, 0.981)	0.762 (0.617, 0.907)	0.806 (0.683, 0.929)
rFOV-DWI ($b=800$ s/mm ²)	0.745 (0.610, 0.880)	0.548 (0.376, 0.720)	0.541 (0.372, 0.710)	0.579 (0.408, 0.750)	0.660 (0.499, 0.821)
fFOV-DWI ($b=0$ s/mm ²)	0.482 (0.311, 0.653)	0.442 (0.275, 0.609)	0.800 (0.680, 0.920)	0.695 (0.548, 0.842)	0.733 (0.598, 0.868)
fFOV-DWI ($b=800$ s/mm ²)	0.613 (0.448, 0.778)	0.527 (0.341, 0.713)	0.669 (0.514, 0.824)	0.713 (0.554, 0.872)	0.683 (0.520, 0.846)

Data are κ values.
Data in parentheses are 95% confidence intervals.
DWI=diffusion weighted imaging, fFOV=full field of view, rFOV=reduced field of view.

5. Discussion

In general, our preliminary study indicated that rFOV-DWI yielded significantly better image quality regarding anatomic detail, distortion, lesion conspicuity, artifacts and overall image quality than fFOV-DWI, especially at $b=800$ seconds/mm² for gastric cancer, and the result is consistent with those in previous reports.^[5,14,24] Moreover, according to previous literature, rFOV-DWI has been applied to various organs and tissues and has achieved high-resolution imaging with a dramatic reduction of susceptibility artifacts.^[14,19,25] Due to the small and narrow shape of the rFOV-DWI scans, some studies have suggested that the pancreas and spinal cord are very suitable for imaging because of their slender anatomic shape.^[19,26] Other studies have suggested that the thyroid gland, prostate, and uterus, which are small organs near the air-tissue boundary, are also well-suited for rFOV-DWI imaging.^[20,22,27] We speculated that the stomach might also be a good target organ because of its anatomic position, which is easily affected by air and motion, especially in the fFOV-DWI scans. Our study is the first study to demonstrate the feasibility of using the rFOV-DWI technique to enhance image quality in scans of individuals with gastric cancer, which may have considerable clinical value in the evaluation of gastric cancer. However, additional studies repeating these methods are still warranted.

The stomach is a hollow moving organ filled with liquid and gas. Movement of the stomach or another intestinal tract and gas may exacerbate artifacts leading to image distortion and ghosting. In addition, concerning the fFOV-DWI sequence, due to the slow traversal via the k-space line and narrow bandwidth along the phase encoding direction, susceptibility artifacts, distortion, and blurring are inevitable.^[10] However, the rFOV-DWI sequence accelerates the traversal and reduces the number of k-space lines by using the 2D echo-planar RF pulse with a shortened readout, which can observably reduce artifacts, distortion and blurring to improve the image quality.^[6,28] Additionally, rFOV-DWI scans with a higher resolution and fewer artifacts have the advantage of revealing the details of gastric cancer by providing more detailed characteristics, such as necrotic, cystic and bleeding within the lesion.^[6,10] Due to the small FOV, the application of rFOV-DWI also reduces the partial volume effect between the tumor and normal tissue, which may result in better lesion conspicuity and anatomic detail, as observed in our study.^[22,25] We think this improvement in image quality might help us increase the sensitivity of diagnoses of small gastric cancers at an early stage and may improve the therapeutic assessments performed after neoadjuvant chemotherapy.

Regarding the 3 parts of the stomach, the average scores of the 2 DWI methods at both b values in various image quality parameters were different. The image quality of the rFOV-DWI scans in the esophagogastric junction was superior to those in the gastric corpus and antrum region. We speculate that the esophagogastric junction may be relatively static and located roughly in the center of the abdomen. When drinking plenty of water, this region is filled, yielding the highest quality of images. However, the quality of the images of the gastric corpus may depend on the degree to which it is filled with water, tumor size, and tumor position. In addition, the gastric antrum is easily influenced by respiratory movement and intestinal movement from the gastric antrum or an adjacent bowel, leading to poor image quality. Overall, the interobserver agreement between 2 observers was relatively good, and the result was convincing.

As for the ADC measurements, we found a significant difference in the average tumor ADC between rFOV-DWI and fFOV-DWI. The mean tumor ADC values of rFOV-DWI were significantly lower than those of fFOV-DWI, which in accordance with the results of previous reports.^[14,20,22] For example, Lu et al^[20] and Barentsz et al^[12] reported that the ADC values calculated from rFOV-DWI scans were significantly smaller than the corresponding values from fFOV-DWI scans in the thyroid glands and breast, respectively. The difference in the ADC values between two sequences is believed to be due to a reduction in the average partial volume in both the tumor and normal tissue with rFOV-DWI, which results in more accurate ADC values.^[22] Moreover, the ADC values from the rFOV-DWI scans may be more precise for evaluating gastric cancer. Other studies found different results.^[6,19,22] For instance, Peng et al^[6] and Kim et al^[19] discovered that there was no significant difference between the average ADC values of both DWI sequences in rectal carcinoma and pancreas, respectively. Numerous factors may influence the ADC values, such as the magnetic field strength, b values, and use of sequence protocols. Furthermore, a reduction in the number of phase encoding steps and the signal-to-noise ratio (SNR) can also lower the ADC values,^[28,29] which are also limitations of this technique. Further evaluations of the ADC measurements from the rFOV-DWI scans are needed.

Our study has several limitations. First, this was a single-center retrospective study, so selection bias may be present. Moreover, the number of patients was relatively small, especially in the analyses of different subgroups based on the tumor location. Future studies with a larger population are warranted to confirm our results. In addition, only 2 b values (0 and 800 seconds/mm²) were used in our study; theoretically, it would be better to measure the value of ADC with multiple b values. Moreover, the rFOV-DWI scans could not cover the entire abdomen, so the detection of lymph nodes or additional gastric metastatic disease indicators is limited, and rFOV-DWI needs to be combined with other sequences. Finally, the ROI drawings were based on the largest plane and may not reflect the entire tumor, which may affect the assessment of the ADC measurements.

6. Conclusion

In conclusion, our study showed that rFOV-DWI yielded significantly better image quality regarding anatomic detail, distortion, lesion conspicuity, artifacts, and overall image quality than fFOV-DWI did. Additionally, the quality of the images obtained by rFOV-DWI in the esophagogastric junction was superior to the quality of the images obtained in the gastric corpus and antrum region. The mean tumor ADC values obtained by rFOV-DWI were significantly lower than those obtained by fFOV-DWI, which may be of value in the clinic.

Author contributions

Conceptualization: Jian-Zhong Sun, Ying Zhou, Ri-Sheng Yu.
Data curation: Jie-Yu Chen, Yuan-Fei Lu, Jian-Zhong Sun, Ying Zhou.

Formal analysis: Jie-Yu Chen, Yuan-Fei Lu, Jian-Zhong Sun, Ying Zhou.

Funding acquisition: Yuan-Fei Lu.

Investigation: Jie-Yu Chen.

Methodology: Hai-Yan Chen, Jie-Yu Chen, Yuan-Fei Lu, Ying Zhou.

Project administration: Hai-Yan Chen.

Resources: Jin-Song Cai, Jie-Yu Chen, Yuan-Fei Lu, Jian-Zhong Sun, Ri-Sheng Yu.

Software: Hai-Yan Chen, Yuan-Fei Lu, Jian-Zhong Sun, Ying Zhou, Ri-Sheng Yu.

Supervision: Jin-Song Cai, Jian-Zhong Sun, Ri-Sheng Yu.

Visualization: Jin-Song Cai, Hai-Yan Chen, Ri-Sheng Yu.

Writing – original draft: Jin-Song Cai.

Writing – review & editing: Hai-Yan Chen.

Ri-Sheng Yu orcid: 0000-0003-0554-9484.

References

- [1] Ferlay J, Soerjomataram I, Dikshit R, et al. Cancer incidence and mortality worldwide: sources, methods and major patterns in GLOBOCAN 2012. *Int J Cancer* 2015;136:E359–86.
- [2] Hohenberger P, Gretschel S. Gastric cancer. *Lancet* 2003;362:305–15.
- [3] Shitara K, Özgüroğlu M, Bang Y-J, et al. Pembrolizumab versus paclitaxel for previously treated, advanced gastric or gastro-oesophageal junction cancer (KEYNOTE-061): a randomised, open-label, controlled, phase 3 trial. *Lancet* 2018;392:123–33.
- [4] Giganti FOE, Esposito A, Chiari D, et al. Prognostic role of diffusion-weighted MR imaging for resectable gastric cancer. *Radiology* 2015;276:444–52.
- [5] Tamada T, Ream JM, Doshi AM, et al. Reduced field-of-view diffusion-weighted magnetic resonance imaging of the prostate at 3 Tesla: comparison with standard echo-planar imaging technique for image quality and tumor assessment. *J Comput Assist Tomogr* 2017;41:949–56.
- [6] Peng Y, Li Z, Tang H, et al. Comparison of reduced field-of-view diffusion-weighted imaging (DWI) and conventional DWI techniques in the assessment of rectal carcinoma at 3.0T: image quality and histological T staging. *J Magn Reson Imaging* 2018;47:967–75.
- [7] Figueiras RG, Goh V, Padhani AR, et al. The role of functional imaging in colorectal cancer. *AJR Am J Roentgenol* 2010;195:54–66.
- [8] Curvo-Semedo L, Lambregts DM, Maas M, et al. Diffusion-weighted MRI in rectal cancer: apparent diffusion coefficient as a potential noninvasive marker of tumor aggressiveness. *J Magn Reson Imaging* 2012;35:1365–71.
- [9] Aoyagi T, Shuto K, Okazumi S, et al. Apparent diffusion coefficient correlation with oesophageal tumour stroma and angiogenesis. *Eur Radiol* 2012;22:1172–7.
- [10] Ma C, Li YJ, Pan CS, et al. High resolution diffusion weighted magnetic resonance imaging of the pancreas using reduced field of view single-shot echo-planar imaging at 3 T. *Magn Reson Imaging* 2014;32:125–31.
- [11] Saritas EU, Cunningham CH, Lee JH, et al. DWI of the spinal cord with reduced FOV single-shot EPI. *Magn Reson Med* 2008;60:468–73.
- [12] Barentsz MW, Tavian V, Chang JM, et al. Assessment of tumor morphology on diffusion-weighted (DWI) breast MRI: diagnostic value of reduced field of view DWI. *J Magn Reson Imaging* 2015;42:1656–65.
- [13] Budzik JF, Vercllyte S, Lefebvre G, et al. Assessment of reduced field of view in diffusion tensor imaging of the lumbar nerve roots at 3 T. *Eur Radiol* 2013;23:1361–6.
- [14] Zhang Y, Holmes J, Rabanillo I, et al. Quantitative diffusion MRI using reduced field-of-view and multi-shot acquisition techniques: validation in phantoms and prostate imaging. *Magn Reson Imaging* 2018;51:173–81.
- [15] Park EH, Lee YH, Jeong EK, et al. Diffusion tensor imaging focusing on lower cervical spinal cord using 2D reduced FOV interleaved multislice single-shot diffusion-weighted echo-planar imaging: comparison with conventional single-shot diffusion-weighted echo-planar imaging. *Magn Reson Imaging* 2015;33:401–6.
- [16] Feng Z, Min X, Sah VK, et al. Comparison of field-of-view (FOV) optimized and constrained undistorted single shot (FOCUS) with conventional DWI for the evaluation of prostate cancer. *Clin Imaging* 2015;39:851–5.
- [17] Sui Y, Arunachalam SP, Arani A, et al. Cardiac MR elastography using reduced-FOV, single-shot, spin-echo EPI. *Magn Reson Med* 2018;80:231–8.
- [18] Xie Y, Li Y, Wen J, et al. Functional evaluation of transplanted kidneys with reduced field-of-view diffusion-weighted imaging at 3T. *Korean J Radiol* 2018;19:201–8.
- [19] Kim H, Lee JM, Yoon JH, et al. Reduced field-of-view diffusion-weighted magnetic resonance imaging of the pancreas: comparison with conventional single-shot echo-planar imaging. *Korean J Radiol* 2015;16:1216–25.
- [20] Lu Y, Hatzoglou V, Banerjee S, et al. Repeatability investigation of reduced field-of-view diffusion-weighted magnetic resonance imaging on thyroid glands. *J Comput Assist Tomogr* 2015;39:334–9.
- [21] Seeger A, Schulze M, Schuettauf F, et al. Advanced diffusion-weighted imaging in patients with optic neuritis deficit - value of reduced field of view DWI and readout-segmented DWI. *Neuroradiol J* 2018;31:126–32.
- [22] Hwang J, Hong SS, Kim HJ, et al. Reduced field-of-view diffusion-weighted MRI in patients with cervical cancer. *Br J Radiol* 1087;91:20170864.
- [23] Vidiri A, Minosse S, Piludu F, et al. Feasibility study of reduced field of view diffusion-weighted magnetic resonance imaging in head and neck tumors. *Acta Radiol* 2017;58:292–300.
- [24] Ota T, Hori M, Onishi H, et al. Preoperative staging of endometrial cancer using reduced field-of-view diffusion-weighted imaging: a preliminary study. *Eur Radiol* 2017;27:5225–35.
- [25] Dong H, Li Y, Li H, et al. Study of the reduced field-of-view diffusion-weighted imaging of the breast. *Clin Breast Cancer* 2014;14:265–71.
- [26] Maki S, Koda M, Ota M, et al. Reduced field-of-view diffusion tensor imaging of the spinal cord shows motor dysfunction of the lower extremities in patients with cervical compression myelopathy. *Spine (Phila Pa 1976)* 2018;43:89–96.
- [27] Korn N, Kurhanewicz J, Banerjee S, et al. Reduced-FOV excitation decreases susceptibility artifact in diffusion-weighted MRI with endorectal coil for prostate cancer detection. *Magn Reson Imaging* 2015;33:56–62.
- [28] Nelles MKR, Gieseke J, Guerland-van Battum MM, et al. Dual-source parallel RF transmission for clinical MR imaging of the spine at 3.0 T: intraindividual comparison with conventional single-source transmission. *Radiology* 2010;257:11.
- [29] Lin JM, Patterson AJ, Chang HC, et al. An iterative reduced field-of-view reconstruction for periodically rotated overlapping parallel lines with enhanced reconstruction (PROPELLER) MRI. *Med Phys* 2015;42:5757–67.